

# Polarization Deficiency and Excess Free Energy of Ion Hydration in Electric Fields

Sergei Gavryushov\* and Per Linse

Physical Chemistry 1, Center for Chemistry and Chemical Engineering, Lund University, P.O. Box 124, S-221 00 Lund, Sweden

Received: January 10, 2003; In Final Form: May 9, 2003

Polarization deficiency and excess ion hydration free energy at an electric field  $E$  (ion hydration free energy at the field  $E$  subtracted by the ion hydration free energy at zero field) of hydrated calcium, sodium, and chloride ions have been determined by Monte Carlo simulations. A spherical cell containing either one ion and molecular water or only molecular water subjected to an external electrical field was used. The permittivity of pure water decreases as  $E$  is increased, in quantitative agreement with previous simulation studies and the Booth theory. The excess ion hydration free energy depends quadratically on  $E$  up to ca.  $2.5 \cdot 10^8$  V/m, whereas it becomes linear in  $E$  at higher field due to dielectric saturation. The values of the excess ion hydration free energies are in quantitative agreement with measured dependencies of the relative permittivity of electrolyte solution upon the ion concentration. A primitive polarization model of electrolyte solution near charged interfaces is proposed. The use of this model leads to an additional effective repulsive force acting on hydrated ions near charged surfaces and significantly affects the distribution of calcium ions near such surfaces.

## Introduction

For the last two decades, electrostatics of highly charged macromolecules has been a subject of growing interest, and extensive modeling of systems containing macroscopic surfaces, colloidal particles, and polymers has been performed. Although all-atom models have been utilized over one decade, all-atom model simulations are still computationally demanding or even unreachable for many macromolecular systems.

Therefore, the primitive model (PM) or the restricted primitive model (RPM) of equal-sized ions are frequently used to describe ionic solutions in contact with charged macromolecules. On this level of modeling, the solvent is represented by a continuous dielectric medium and the ions by charged hard spheres. The description of the charged macromolecules is also normally coarse-grained. The PM is solved either by simulation techniques or by theoretical methods. The former provides essentially exact solutions of the PM, whereas liquid state theories and the Poisson–Boltzmann (PB) equation provide approximate solutions of the model system but require significantly less numerical effort.

The primitive model has shown to be a well-balanced model able to explain a number of physicochemical properties of systems containing highly charged macromolecules.<sup>1</sup> The model, e.g., has been able to account for the charge stabilization of suspensions of charged colloids,<sup>2,3</sup> special properties of polyelectrolyte solutions as compared to polymer solutions,<sup>4</sup> and  $pK$  values of protein ionizable groups and energy of protein–ligand interactions.<sup>5–14</sup>

Nevertheless, there are also ample of situations where the primitive model fails to provide an accurate description of experimental results. (i) Pronounced ion-specific ability to precipitate charged macromolecules has been documented and leads to the concept of the Hofmeister or the lyotropic series.<sup>15</sup> It seems unlikely that the only parameter available, the hard-core radius, can explain ion specificity for all phenomena of

protein stability, DNA–protein interactions, and ion transport. (ii) Short-range attraction between double helices of DNA in the presence of some multivalent counterions<sup>16</sup> has been experimentally observed. To explain this phenomenon as well as supercoiling of DNA,<sup>17</sup> additional “hydration” forces have been introduced.<sup>16–18</sup> The link between these ion-specific forces and the double-layer theories of electrolyte is still far from clarity, although Monte Carlo simulations using the PM revealed attraction due to interionic correlation effects between two charged planar surfaces<sup>19</sup> and for cylindrically averaged model of DNA.<sup>20</sup> In recent simulation studies, similar attractions between spherical macroions have been observed in solutions of equally charged macroions with multivalent counterions.<sup>21,22</sup> Molecular dynamics simulations of DNA–DNA interactions using the RPM and an explicit charge pattern model of DNA reveal a short-range attraction at some mutual orientations of the two double helices even in the case of monovalent counterions.<sup>23</sup> So, the applicability of the PM should be verified in the case of so highly charged polyanions as DNA.

Many attempts have been made to improve the PM. For example, efforts have been made to include ion hydration forces,<sup>24</sup> dispersion potentials,<sup>25</sup> and field-dependent permittivity arising from external field and dissolved simple ions.<sup>26</sup> In the following, we will in more detail discuss the last issue.

In aqueous solution, water molecules near an ion form a hydration shell. These water molecules are strongly oriented by the electric field of the ion;<sup>27–32</sup> in the case of a divalent or trivalent cations, the orientational effect pertains also water molecules in the second coordination shell.<sup>33–36</sup> As follows from explicit solvent simulations, hydration shells exhibit a structural stability at external electric fields up to ca.  $2 \text{ V/Å}$ ,<sup>37</sup> and hence the polarization of the hydrated water molecules in this field is different from polarization of the same number of water molecules in bulk.<sup>38</sup> As a result, the potential of mean force acting on this hydrated ion in the external electric field should include the free energy of polarization of this highly ion-specific hydration shell. Actually, the ion together with its coordinated

\* Corresponding author. E-mail: Sergei.Gavryushov@fkem1.lu.se.

water can be described as a spherical depression of permittivity<sup>33,39</sup> due to near dielectric saturation. This effect leads to the experimentally measured decrease of the dielectric constant of electrolyte as the ionic concentration is increased.<sup>40–45</sup> The lower polarization of a hydration shell in comparison with the surrounding water causes an additional repulsion of the ion from the high electric field created by a macromolecule or charged surface. Also the dielectric saturation effects might be of importance to the electron-transfer processes.<sup>46</sup>

In a recent work,<sup>47</sup> the dielectric depression, together with the dependence of the dielectric constant of electrolyte upon the ion concentrations and electric field intensity, was estimated from experimental data and incorporated into a model solved using the modified Poisson–Boltzmann equations. With divalent counterions, the ion distribution and mean potential around a charged cylinder representing DNA were found to be sensitive to the lower polarization of the ion hydration shell and notably different from PM results. That study raised questions about the importance of the polarization free energy of ion hydration shells as a function of the electric field.

In the present work, Monte Carlo simulations of solvated calcium, sodium, and chloride ions in the external field have been performed. The polarization deficiency and excess ion hydration free energies are obtained for several intensities of an external electric field. The range of field intensity involves all cases expected for the charged macromolecules and bilayers. The predicted decrease of electrolyte permittivity as a function of ion concentration is compared to experimental data. Finally, a primitive polarization model is proposed, being an improvement of the primitive model for electrolyte solutions, and applied to DNA in salt solution.

## Model

**Hydration of a Single Ion.** Two model systems are used to obtain Helmholtz free energy of ion hydration as a function of the strength of an external electric field. System 1 consists of a spherical cell of water molecules (left part of Figure 1), and system 2 of a spherical cell of water molecules plus an ion fixed at the center of the sphere (right part of Figure 1). The spherical cells have the common radius  $R_{\text{cell}}$  and are imbedded into a dielectric continuum with the relative permittivity  $\epsilon$ . The spherical cells will be subjected to an external and homogeneous electrical field  $\mathbf{E}$ .

Let  $H_{\alpha}^0$  ( $\alpha = 1, 2$ ) denote the Hamiltonian of system  $\alpha$  in the absence of the electric field. The Hamiltonian of system  $\alpha$  in the presence of the electric field  $\mathbf{E}$ ,  $H_{\alpha}(E)$ , can be divided into three contributions according to

$$H_{\alpha}(E) = H_{\alpha}^0 + H_{\alpha}^{\text{mol}}(E) + H_{\alpha}^{\text{diel}}(E) \quad (1)$$

where  $H_{\alpha}^{\text{mol}}(E) = -\mathbf{P}_{\alpha}(\mathbf{E}) \cdot \mathbf{E}_{\text{cav}}$  describes the coupling between the molecular system and the electric field, with  $\mathbf{P}_{\alpha}$  denoting the induced dipole moment of the molecular system, and  $H_{\alpha}^{\text{diel}}(E)$  describes the polarization of the dielectric continuum surrounding the spherical cell by the field. The electric field inside a spherical cavity in a dielectric continuum with the relative permittivity  $\epsilon(E)$ , to which a homogeneous field  $\mathbf{E}$  is applied, is given by  $\mathbf{E}_{\text{cav}} = \{3\epsilon(E)/[2\epsilon(E) + 1]\}\mathbf{E}$ .<sup>48</sup>

Conceptually, the free energy difference  $\Delta F_{\text{hydr}}(0) \equiv F_2(0) - F_1(0)$ , where  $F_1(0)$  and  $F_2(0)$  are the free energies of system 1 and 2 at  $E = 0$ , respectively, constitutes the free energy of hydrating the ion in the absence of the external field (upper part of Figure 1). On the molecular level,  $\Delta F_{\text{hydr}}(0)$  involves several contributions including favorable ion–water interaction

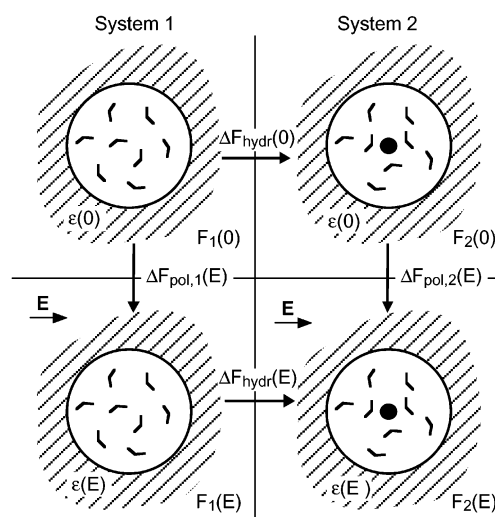


**Figure 1.** Schematic illustration of the model systems and thermodynamic cycle used. A spherical cavity surrounded by a dielectric medium contains water molecules (system 1, left) or water molecules plus an ion (system 2, right) either in the absence (top) or in the presence (bottom) of an external electric field  $\mathbf{E}$ . The central quantity  $\Delta\Delta F(E)$ , denoting the ion hydration free energy at the field  $E$  in excess to that at  $E = 0$ , can be expressed as  $\Delta F_{\text{hydr}}(E) - \Delta F_{\text{hydr}}(0)$  or as  $\Delta F_{\text{pol},2}(E) - \Delta F_{\text{pol},1}(E)$ , of which the latter expression is computationally advantageous. See text for further details.

and free energy loss associated with broken hydrogen bonds and water ordering. In the presence of an external field  $\mathbf{E}$ , the hydration free energy becomes field dependent according to  $\Delta F_{\text{hydr}}(E) \equiv F_2(E) - F_1(E)$ , where  $F_1(E)$  and  $F_2(E)$  denote the free energies of system 1 and 2, respectively, in the presence of the field (lower part of Figure 1). The ion hydration free energy at the field  $\mathbf{E}$  in excess to the ion hydration free energy at zero field is now defined according to

$$\Delta\Delta F(E) \equiv \Delta F_{\text{hydr}}(E) - \Delta F_{\text{hydr}}(0) = [F_2(E) - F_1(E)] - [F_2(0) - F_1(0)] \quad (2)$$

On the basis of the model, the aim is to derive an expression of  $\Delta\Delta F(E)$  suitable for numerical evaluation. Following the division of the field-dependent part of the Hamiltonian into two terms,  $\Delta\Delta F(E)$  can be expressed as

$$\Delta\Delta F(E) = \Delta\Delta F^{\text{mol}}(E) + \Delta\Delta F^{\text{diel}}(E) \quad (3)$$

where  $\Delta\Delta F^{\text{mol}}(E)$  is the contribution from the molecular part and  $\Delta\Delta F^{\text{diel}}(E)$  from the surrounding dielectric.

The molecular contribution to  $\Delta\Delta F(E)$  can formally be expressed as

$$\Delta\Delta F^{\text{mol}}(E) = \Delta F_{\text{pol},2}^{\text{mol}}(E) - \Delta F_{\text{pol},1}^{\text{mol}}(E) \quad (4)$$

with  $\Delta F_{\text{pol},\alpha}(E)$  denoting the free energy of polarizing system  $\alpha$  by the external field according to  $\Delta F_{\text{pol},\alpha}(E) \equiv F_{\alpha}(E) - F_{\alpha}(0)$  (see left and right parts of Figure 1). With the use of thermodynamic integration,  $\Delta F_{\text{pol},\alpha}^{\text{mol}}(E)$  can be written as

$$\Delta F_{\text{pol},\alpha}^{\text{mol}}(E) = \int_0^E \left\langle \frac{\partial H_{\alpha}^{\text{mol}}(E')}{\partial E'} \right\rangle dE' \quad (5)$$

where  $H_{\alpha}^{\text{mol}}(E)$  is the molecular part of the Hamiltonian of system  $\alpha$  depending on the electric field  $E$ . With the use of the expressions for  $H_{\alpha}^{\text{mol}}(E)$  and  $E_{\text{cav}}$  given below eq 1 as well as eqs 4 and 5,  $\Delta\Delta F^{\text{mol}}(E)$  can be expressed as

$$\Delta\Delta F^{\text{mol}}(E) = -\int_0^E [P_2(E') - P_1(E')] \frac{3\epsilon(E')}{2\epsilon(E') + 1} dE' \quad (6)$$

where  $\mathbf{P}_\alpha$  being parallel to  $\mathbf{E}$  has been assumed. Typically,  $\Delta\Delta F^{\text{mol}}(E)$  is positive since the ability of the field to polarize water molecules near an ion is smaller than in bulk due to the ordering of the water molecules by the electric field of the ion. Hence, the difference in the induced total dipole moment  $\Delta P(E) \equiv P_2(E) - P_1(E)$  is negative, and it will be referred to as a polarization deficiency of the ion hydration shell as compared to the corresponding volume of bulk water.

The dielectric contribution to  $\Delta F_{\text{hydr}}(E)$  can be regarded as the change of the polarization free energy of the surrounding dielectric during the charging process of the ion at the field  $E$ . Hence,  $\Delta\Delta F^{\text{diel}}(E)$  can be approximated as

$$\Delta\Delta F^{\text{diel}}(E) \approx \frac{Q^2}{8\pi\epsilon_0 R_{\text{cell}}} \left[ \frac{1}{\epsilon(E)} - \frac{1}{\epsilon(0)} \right] \quad (7)$$

where it is assumed that the electric field created by the ion at distance  $R_{\text{cell}}$  is much smaller than  $E$  and  $Q$  denotes the ion charge. Since  $\epsilon(E) < \epsilon(0)$ ,  $\Delta\Delta F^{\text{diel}}(E)$  is also positive. At small  $E$ , the field dependence of the relative permittivity can be expanded to the second-order  $\epsilon(E) = \epsilon(0)(1 - \gamma E^2)$ ,<sup>48</sup> which inserted into eq 7 gives  $\Delta\Delta F^{\text{diel}}(E) = [Q^2/8\pi\epsilon_0\epsilon(0)R_{\text{cell}}]\gamma E^2$ .

Providing that (i) the electric field inside a sphere of water without the ion is homogeneous (system 1) and (ii) a radius of this sphere is notably larger than the ion hydration shell (system 2), the field  $\mathbf{E}$  and the polarization  $\mathbf{P}(\mathbf{E})$  can be calculated for a spherical cell of water molecules surrounded with nonpolarizable dielectric medium ( $\epsilon = 1$ ) and placed into the external field  $\mathbf{E}_0$ . At a weak field, it is expected that  $\mathbf{E} \rightarrow \{3/[(2 + \epsilon(0))]\mathbf{E}_0$ .

A slight complication appears due to the fact that water molecules near the cell surface are perturbed by the surface. Therefore, the electric field  $E$  and the induced dipole moments  $P_1(E)$  and  $P_2(E)$  should be averaged using an inner sphere with the radius  $R_{\text{pol}} < R_{\text{cell}}$ , and the dielectric contribution should be applied from  $R_{\text{pol}}$  ( $R_{\text{cell}}$  substituted by  $R_{\text{pol}}$  in eq 7). Ideally,  $\Delta\Delta F(E)$  should not significantly depend on the precise value of  $R_{\text{pol}}$ .

**Homogeneous Electrolyte Solution.** If we consider some volume  $V$  of a homogeneous electrolyte solution placed in a weak homogeneous external electric field, where linear dielectric response applies, the chemical potential of ion  $i$  depends on  $\mathbf{E}$  according to

$$\Delta\mu_i(E) \equiv \left( \frac{\partial \Delta F(E)}{\partial N_i} \right)_{T,D,N_{j \neq i}} \approx \left( \frac{\partial (VD^2/2\epsilon\epsilon_0)}{\partial N_i} \right)_{T,D,N_{j \neq i}} = -\frac{\epsilon_0}{2} \left( \frac{\partial \epsilon}{\partial n_i} \right)_{T,D,N_{j \neq i}} E^2 \quad (8)$$

where  $\Delta\mu_i(E)$  is a part of the chemical potential of ion species  $i$  depending upon  $E$ ,  $\Delta F(E)$  the  $E$ -dependent part of the free energy of the electrolyte,  $N_i$  the number of ions of type  $i$ ,  $D$  the electrical displacement, and  $n_i = N_i/V$ . According to experimental data obtained by extrapolation of the 1 GHz impedances to zero frequency,<sup>40–43</sup> the permittivity of electrolyte solutions is decreasing linearly at increasing ion concentrations up to  $c \approx 4$  M as

$$\epsilon(c) = \epsilon_w - \sum_i \delta_i c_i \quad (9)$$

**TABLE 1: Lennard-Jones Parameters  $\sigma$  and  $\epsilon$  for SPC(E) Water and Some Ions<sup>a</sup>**

atom/ion	$\sigma$ (Å)	$\epsilon$ (kJ/mol)
O	3.1655 <sup>b</sup>	0.650 <sup>b</sup>
Ca <sup>2+</sup>	2.361 <sup>c</sup>	1.88 <sup>c</sup>
Na <sup>+</sup>	3.328 <sup>c</sup>	0.0116 <sup>c</sup>
Na <sup>+</sup>	2.584 <sup>d</sup>	0.418 <sup>d</sup>
Cl <sup>−</sup>	4.40 <sup>e</sup>	0.418 <sup>e</sup>

<sup>a</sup> Ion–water oxygen parameters were obtained using Lorentz–Berthelot mixing rules. <sup>b</sup> Ref 49. <sup>c</sup> Ref 50. <sup>d</sup> Ref 52. <sup>e</sup> Ref 51.

where  $\epsilon_w$  is the relative permittivity of pure water. After the identification  $\Delta\Delta F_i(E) = \Delta\mu_i(E)$  and the use of eqs 8 and 9, the dependence of  $\Delta\Delta F_i(E)$  on  $E$  at low electric fields can be expressed as

$$\Delta\Delta F_i(E) = \alpha_i E^2 \quad (10)$$

where

$$\alpha_i = \frac{\epsilon_0}{2} \delta_i \quad (11)$$

(Note,  $\delta_i$  is typically given in M<sup>−1</sup> so the conversion factor 1/1000 $N_A$ , with  $N_A$  being Avogadro's number has to be applied in eq 11 to convert to SI units). Hence, the excess ion hydration free energy  $\Delta\Delta F_i(E)$  at low field strength, where it depends quadratically on  $E$ , can be related to experimental  $\delta_i$  values through eqs 10 and 11.

## Details of the Simulations

The free energy of the ion hydration has been examined for Ca<sup>2+</sup>, Na<sup>+</sup>, and Cl<sup>−</sup> ions. Water molecules were represented using the SPC/E water model.<sup>49</sup> The Ca<sup>2+</sup>–water and Na<sup>+</sup>–water potentials were taken from Åqvist,<sup>50</sup> who has provided a set of SPC water–alkali ion and SPC water–alkali earth metal ion potentials being successful in prediction of hydration free energies. We have confirmed that negligible deviation from SPC water hydration free energies for Ca<sup>2+</sup> and Na<sup>+</sup> are obtained using the SPC/E water potential. The Cl<sup>−</sup>–water potential was taken from Smith and Dang.<sup>51</sup> Finally, the Na<sup>+</sup>–water by Dang<sup>52</sup> was also used in few occasions to examine the sensitivity on the ion–water potential models. The Lennard-Jones parameters of the water–water and ion–water interactions are summarized in Table 1.

In both system 1 and 2, the spherical cell contained 500 water molecules and the cell had the radius  $R_{\text{cell}} = 15.3$  Å. No reaction field was applied; i.e., the medium surrounding the cell was approximated by vacuum. The temperature was  $T = 298$  K throughout.

The properties of the model systems were obtained by performing Monte Carlo (MC) simulations. Dielectric properties are known to display a slow convergence, and extensive simulations were needed to obtain results of sufficient precision. For each system and at each field strength,  $N$  separate simulations each involving  $20\,000 \times M$  trial moves per particle were performed after equilibration comprising 20 000 trial moves. Such a separation allowed us to do the  $N$  simulations in parallel applying different sequences of random numbers to the MC procedure. Here,  $N = 8$  (pure water and Ca<sup>2+</sup> solution) and 16 (Na<sup>+</sup> and Cl<sup>−</sup> solutions) were used, and  $M$  varied from 20 (Na<sup>+</sup> and Cl<sup>−</sup> solutions) and 40 (pure water and Ca<sup>2+</sup> solution) at  $E_0 = 0.66$  V/Å to 80 (Na<sup>+</sup> and Cl<sup>−</sup> solutions) and 160 (pure water and Ca<sup>2+</sup> solution) at  $E_0 = 0.22$  V/Å. Reported uncertainties are two standard deviations, and they were evaluated using the



**TABLE 2: Averaged Electric Field  $E$ , Averaged Water Polarization  $p$ , and Calculated Water Permittivity  $\epsilon$  at Different External Field  $E_0$ <sup>a</sup>**

$E_0$ (V/Å)	$10^2 \cdot E$ (V/Å)			$10^3 \cdot p$ (e/Å <sup>2</sup> )			$\epsilon$		
				$R_{\text{pol}}$					
	6 Å	8 Å	11 Å	6 Å	8 Å	11 Å	6 Å	8 Å	11 Å
0.22	1.0(2)	1.0(1)	0.9(1)	3.6(1)	3.66(7)	3.67(4)	67(13)	67(9)	71(7)
0.44	2.7(2)	2.6(1)	2.5(1)	7.9(1)	7.9(1)	7.97(4)	54(6)	56(4)	59(3)
0.55	4.3(3)	4.4(2)	4.4(1)	10.2(1)	10.15(6)	10.12(4)	44(3)	43(2)	43(1)
0.66	7.5(3)	7.7(2)	7.6(1)	12.2(2)	12.06(6)	11.92(3)	31(2)	29.3(8)	29.4(5)

<sup>a</sup> The spherical cell has the radius  $R_{\text{cell}} = 15.3$  Å, contains 500 SPC/E water molecules, and is immersed into nonpolarizable medium.  $E$  and  $p \equiv P/V_{\text{pol}}$  are spatially averaged over spheres with different radii  $R_{\text{pol}}$  and  $\epsilon = p/\epsilon_0 E + 1$ .

results from the  $N$  separate simulations. All simulations were carried out employing the MOLSIM package.<sup>53</sup>

The spatial averages of the electric field  $E$  and the total dipole moment  $P$  projected onto  $E_0$  were calculated for three spheres with radii  $R_{\text{pol}} = 6, 8$ , and  $11$  Å with the corresponding volumes  $V_{\text{pol}} = (4\pi/3)R_{\text{pol}}^3$ . The spatially averaged electric field was calculated according to  $E_z = E_0 - \langle \psi/z \rangle$  (assuming that  $E_0$  is directed along the  $z$  axis), where  $\psi$  is the electrostatic potential created by other molecules in the center of the oxygen atom of a water molecule. Here,  $\langle \dots \rangle$  denotes an averaging over all water molecules at  $r < R_{\text{pol}}$ , but excluding those in a thin layer  $|z| \leq 1$  Å for numerical reasons. The values of the external field  $E_0$  were 0.22, 0.44, 0.55, and 0.66 V/Å. The smallest  $E_0$  corresponded to  $E \approx 0.01$  V/Å inside the sphere of water molecules for  $\epsilon \approx 70$  (the dielectric constant of SPC/E water).<sup>54</sup>

Previous simulations of water at high electric fields<sup>55</sup> indicated that the distortion of the water density distribution might appear up to 7 Å from a water surface. In the present study, no significant difference among the dielectric results for the three different  $R_{\text{pol}}$  was found. Nevertheless, the final results for  $R_{\text{pol}} = 11$  Å (system 2) are excluded due to their large uncertainties.

## Simulation Results

**Permittivity.** The polarization of the sphere containing water only (system 1) will first be considered. Table 2 shows the spatially averaged electric field  $E$ , the averaged water polarization  $p \equiv P/V_{\text{pol}}$  and the extracted relative permittivity  $\epsilon = p/\epsilon_0 E + 1$  for the SPC/E water from the simulations using the three different radii  $R_{\text{pol}}$  for sampling of the electric field and the water polarization. There is generally a good agreement among the results for the different  $R_{\text{pol}}$ , and the uncertainties decrease as  $R_{\text{pol}}$ , and hence  $V_{\text{pol}}$ , is increased.

Figure 2 shows the relative permittivity  $\epsilon$  as a function of the electric field  $E$ . There is a good agreement among (i)  $\epsilon(E)$  using water enclosed in a sphere at an external electric field (present study), (ii)  $\epsilon(E)$  using water enclosed between two planar surfaces at an external electric field by Yeh and Berkowitz,<sup>55</sup> and (iii)  $\epsilon(E = 0)$  determined from total dipole moment fluctuations by Svishchev and Kusalik,<sup>54</sup> all using the SPC/E water model. Thus, this verifies the present approach of calculating the polarization of molecular water in a spherical cavity. In addition, it should be noticed that all simulation results confirm the Booth theory derived more than half a century ago.<sup>56</sup>

In the following, the data for  $R_{\text{pol}} = 8$  Å are used to characterize the dielectric properties of pure water.

**Polarization Deficiency.** The polarization deficiency of the ion hydration shell as compared to the corresponding volume of water will now be considered. Figure 3 displays  $\Delta P(E)$  as a function of  $E$  for the three different ions examined using  $R_{\text{pol}} = 6$  and  $8$  Å. Starting with  $\text{Ca}^{2+}$ , Figure 3 shows that the water polarization deficiency increases linearly up to  $E \approx 0.025$  V/Å, whereas at higher electrical field,  $\Delta P$  levels off. The corre-

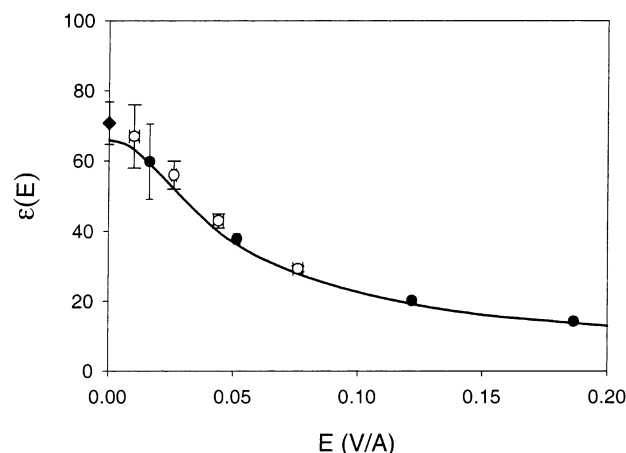


**Figure 2.** Relative water permittivity  $\epsilon(E)$  as a function of the intensity of electric field  $E$  from the present study (open circles), molecular dynamics simulations in ref 55 (filled circles), a zero field result in ref 54 (diamond), and the Booth theory using  $\mu_{\text{water}} = 1.85$  D, ref 56 (solid curve).

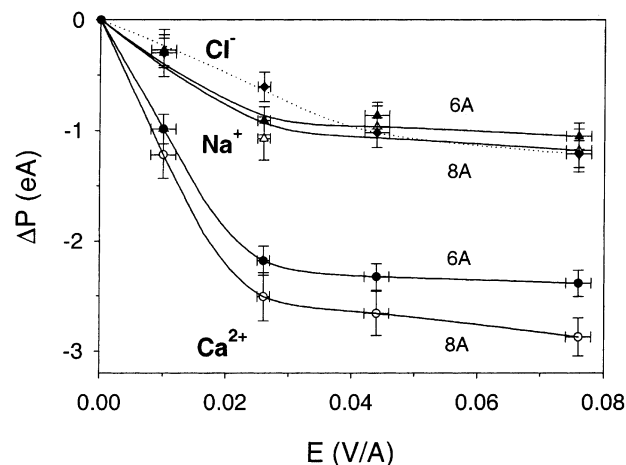


**Figure 3.** Polarization deficiency of the ion hydration shell  $\Delta P(E)$  as a function of the intensity of electric field  $E$  for  $\text{Ca}^{2+}$  (circles),  $\text{Na}^+$  (triangles), and  $\text{Cl}^-$  (diamonds) using  $R_{\text{pol}} = 6$  (filled symbols) and  $8$  Å (open symbols). For clarity data for  $\text{Cl}^-$ ,  $R_{\text{pol}} = 8$  Å has been omitted. The curves are only a guide for the eye.

sponding polarization deficiency of the monovalent ions is smaller. The trends are similar with an initial linear regime and a saturation at higher electric field. Within the statistical uncertainties, the data for  $\text{Na}^+$  and  $\text{Cl}^-$  are the same; possibly at  $E = 0.026$  V/Å, a smaller polarization deficiency appears for  $\text{Cl}^-$ . Thus, the results display the expected trend that the polarization deficiency is larger for divalent ions as compared to monovalent ones. Hence, the stronger electrostatic field of the divalent ions has a larger impact on the orientation of nearby water molecules with respect to the ion–water vector, reducing

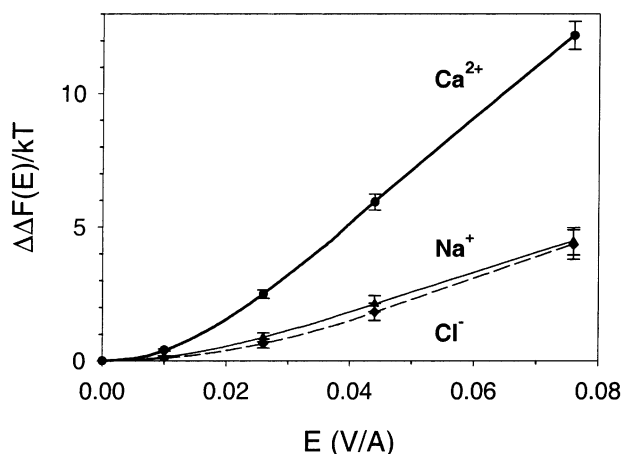


**Figure 4.** Excess ion hydration free energy  $\Delta\Delta F(E)$  as a function of the intensity of the electric field  $E$  for  $\text{Ca}^{2+}$  (circles),  $\text{Na}^+$  (triangles), and  $\text{Cl}^-$  (diamonds) using  $R_{\text{pol}} = 6 \text{ \AA}$ . The curves are only a guide for the eye.

**TABLE 3: Excess Ion Hydration Free Energy  $\Delta\Delta F(E)$  (kT) (See Eqs 3, 6, and 7) for Calcium, Sodium, and Chloride Ions**

$E$ (V/Å)	$\text{Ca}^{2+}$		$\text{Na}^{+}$		$\text{Cl}^{-}$	
	$R_{\text{pol}}$					
	6 Å	8 Å	6 Å	8 Å	6 Å	8 Å
0.01	0.41(4)	0.45(6)	0.15(4)	0.15(7)	0.10(4)	0.11(6)
0.026	2.5(2)	2.7(3)	0.9(2)	0.9(3)	0.7(2)	0.7(3)
0.044	6.0(3)	6.2(5)	2.1(3)	2.2(5)	1.8(3)	1.8(5)
0.077	12.2(5)	12.7(8)	4.5(5)	4.6(8)	4.4(6)	4.4(9)

the ability of these water molecules to become polarized by the external field.

Moreover, Figure 3 also shows that the polarization deficiency becomes larger for  $R_{\text{pol}} = 8 \text{ \AA}$  as compared to  $R_{\text{pol}} = 6 \text{ \AA}$ . Thus, there is a significant contribution to the deficiency beyond the first hydration shell, which extends to 3.5, 3.7, and 3.9  $\text{\AA}$  for  $\text{Ca}^{2+}$ ,  $\text{Na}^+$ , and  $\text{Cl}^-$ , respectively, as deduced from their ion–water radial distribution functions.

**Excess ion Hydration Free Energy.**  $\Delta\Delta F(E)$  has been obtained by integrating the polarization deficiency (eq 6) and applying the surrounding dielectric contribution (eq 7 taken with  $R_{\text{cell}}$  substituted by  $R_{\text{pol}}$ ) according to eq 3. Figure 4 displays  $\Delta\Delta F(E)$  graphically using  $R_{\text{pol}} = 6 \text{ \AA}$ . As alluded to in the model section,  $\Delta\Delta F(E)$  is positive and grows quadratically at small  $E$ . For  $\text{Ca}^{2+}$ , the excess ion hydration free energy amounts to one  $kT$  at  $E = 0.015 \text{ V/\AA}$  and becomes 12  $kT$  at  $E = 0.077 \text{ V/\AA}$ . Regarding the monovalent counterions,  $\Delta\Delta F(E)$  amounts to one  $kT$  at  $E \approx 0.03\text{--}0.04 \text{ V/\AA}$ . Thus, the excess ion hydration free energy can be considerable, and its consequences will be illustrated in the next section.

Table 3 provides the numerical values of  $\Delta\Delta F(E)$  using  $R_{\text{pol}} = 6$  and 8  $\text{\AA}$ . The addition of the analytic  $\Delta\Delta F^{\text{diel}}(E, R_{\text{pol}})$  to the simulated  $\Delta\Delta F^{\text{mol}}(E, R_{\text{pol}})$  brings  $\Delta\Delta F(E)$  for the both  $R_{\text{pol}}$  radii to agree within the statistical uncertainties. The magnitude of the continuum dielectric term is not negligible; for  $\text{Ca}^{2+}$  the correction is  $0.9kT$  at  $E = 0.077 \text{ V/\AA}$  and  $R_{\text{pol}} = 6 \text{ \AA}$ . Hence, the continuum correction is necessary and appears to be applicable already from  $\approx 6 \text{ \AA}$ . The statistical uncertainty of  $\Delta P(E)$  and hence  $\Delta\Delta F(E)$  increase as  $R_{\text{pol}}$  is increased, suggesting that  $R_{\text{pol}}$  should not be selected unnecessarily large.

In the present study, only dipole polarization arising from orientation polarization of the water molecules is taken into account. Thus, (i) the nucleus and electronic polarization of the

**TABLE 4: Values of  $\delta_i \text{ (M}^{-1}\text{)}$  (See Eq 9) for Calcium, Sodium, and Chloride Ions from Simulations and Deduced from Experiments**

ion	simulations <sup>a</sup>	experiment	
		ref 40 <sup>b</sup>	ref 41 <sup>c</sup>
$\text{Ca}^{2+}$	24(2)		27(2)
$\text{Na}^+$	8(2)	8(1)	10(2)
$\text{Cl}^-$	5(3)	3(1)	0(2)

<sup>a</sup> Evaluated from the quadratic dependence of  $\Delta\Delta F(E)$  at small  $E$ .

<sup>b</sup> From measured  $-\text{d}\epsilon(c)/\text{d}c = 11(1) \text{ M}^{-1}$  for NaCl and an argument that  $\delta_{\text{Na}^+} \gg \delta_{\text{Cl}^-}$ . <sup>c</sup> From measured  $-\text{d}\epsilon(c)/\text{d}c = 10(2) \text{ M}^{-1}$  for NaCl and  $27(2) \text{ M}^{-1}$  for  $\text{CaCl}_2$  supplemented with the assumption  $\delta_{\text{Cl}^-} = 0$ .

water molecules and (ii) the electronic polarization of the ions are neglected. The effects of the former ones could be small due to a substantial degree of cancellation, since they are neglected both in systems 1 and 2. However, similar simulation studies with polarizable water models have to be performed for assessing this effect. Ion polarization is more important for anions, as compared to cations, owing to larger electronic polarization. The electronic polarizability of  $\text{Cl}^-$  in solution is about  $3.7\text{--}4.0 \text{ \AA}^3$ ,<sup>57–59</sup> which, however, would decrease the excess free energy of a hydrated chloride ion only by about 1% at  $E = 0.01 \text{ V/\AA}$ . Thus, we conclude that the ion electronic polarization can be neglected even in the case of the more polarizable  $\text{Cl}^-$  anion.

The  $\text{Na}^+$ –water potential by Dang<sup>52</sup> was also used. The difference in  $\Delta P$  at  $E = 0.077 \text{ V/\AA}$  between simulations using Dang’s and Åqvist’s  $\text{Na}^+$ –water potentials was a few percent and smaller than the statistical uncertainty.

**Salt Dependency of the Relative Permittivity.** According to eqs 9–11, the excess free energy of ion hydration can be used to determine how the relative permittivity depends on the ion concentration by using the initial quadratic dependency of  $\Delta\Delta F(E)$  on  $E$ . The  $\delta_i$  values obtained are compiled in Table 4. Chandra<sup>60</sup> and Zasetky and Svishchev<sup>39</sup> have recently determined the dependence of SPC/E water permittivity on the NaCl concentration at  $T = 298 \text{ K}$  by direct sampling of the mean square dipole moment fluctuations at different salt concentrations. They obtained  $\delta_{\text{NaCl}} \approx 12$  and  $10 \text{ M}^{-1}$ , respectively, in close agreement with  $\delta_{\text{Na}^+} + \delta_{\text{Cl}^-} = 13(4) \text{ M}^{-1}$  from the present study. These model predictions should be compared with recent experimental data  $\delta_{\text{NaCl}} = 12.8(4) \text{ M}^{-1}$  by Buchner et al.<sup>43</sup> A respectable agreement is hence found between experiment and simulations.

Experimentally, individually  $\delta_i$  cannot be determined without assumptions. However, in some earlier experimental studies, individual  $\delta_i$  was suggested after applying some auxiliary arguments. Such individual  $\delta_i$  values reported by Hasted et al.<sup>40</sup> and Harris and O’Konski<sup>41</sup> are given in Table 4, and in both studies,  $\delta_{\text{Na}^+} \gg \delta_{\text{Cl}^-}$  was suggested. Unfortunately, the precision of the simulation data does not allow an assessment of those results.<sup>61</sup>

### Primitive Polarization Model of Electrolyte Solution

The present simulations have shown that the hydration free energy depends significantly on an external electric field; for  $\text{Ca}^{2+}$  the hydration free energy exceeds one  $kT$  at  $E = 0.015 \text{ V/\AA}$ . An electric field of such intensity appears, e.g., in the vicinity of DNA at physiological conditions, surfactant bilayers, vesicles, and micelles. In the following, we propose an extension of the primitive model, in which polarization effects are incorporated. This model will be called the primitive polarization model (PPM), and it will be applied to describe the ion distribution in solution near DNA.

**Description of the Model.** There are strong evidences that ions retain their first hydration shell even in contact with charged macromolecules. This guides us to divide the hydration shell of an ion into two regions: (i) a spherical region extending from the center of the ion to  $r = R_{\text{diel}}$  and (ii) a remaining outer region. In the inner region ( $r < R_{\text{diel}}$ ), the polarization is described explicitly, whereas in the outer one ( $r > R_{\text{diel}}$ ), the solvent is described as a continuum with the relative permittivity dependent on the electric field and the ion concentration  $\epsilon(E, c)$ . This approach was initially considered in works by Prigogine, Mazur, and Defay,<sup>62</sup> Bolt,<sup>63</sup> Sparnaay,<sup>64</sup> and Levine.<sup>65</sup>

An average relative permittivity of an ion hydration shell can be estimated as long as  $\Delta P(E)$  depends linearly, and hence  $\Delta\Delta F(E)$  quadratically, on  $E$  (e.g.,  $E < 0.025 \text{ V/\AA}$  for hydration of  $\text{Ca}^{2+}$ , see Figure 3). The dielectric property of the inner polarization region will be represented by that of a dielectric sphere with the relative permittivity  $\epsilon_i$ . The values of  $\epsilon_i$  and  $R_{\text{diel}}$  are ion-specific, and  $\epsilon_i$  can be determined from  $\Delta\Delta F(E)$  as follows. The excess ion hydration free energy associated with the inner region  $\Delta\Delta F(E, R_{\text{diel}})$  can be expressed as the contribution from the excess hydration free energy of  $\Delta\Delta F(E)$  subtracted by the contribution from the outer region  $\Delta\Delta F_c(E, R_{\text{diel}})$  according to

$$\Delta\Delta F(E, R_{\text{diel}}) = \Delta\Delta F(E) - \Delta\Delta F_c(E, R_{\text{diel}}) \quad (12)$$

with  $\Delta\Delta F_c(E, R_{\text{diel}})$  approximated by the continuum description given by eq 7. By equalizing  $\Delta\Delta F(E, R_{\text{diel}})$  with the polarization free energy of the spherical cavity

$$\Delta\Delta F_i^{\text{cav}}(E, R_{\text{diel}}) = \left( \frac{4\pi R_{\text{diel}}^3}{3} \right) \frac{\epsilon_0}{2} \frac{3\epsilon_w(\epsilon_w - \epsilon_i)}{2\epsilon_w + \epsilon_i} E^2 \quad (13)$$

$\epsilon_i$  is obtained. For latter use,  $\Delta\Delta F(E, R_{\text{diel}})$  can also be expressed in terms of  $\delta(R_{\text{diel}})$  through eqs 10 and 11. For sufficiently small  $R_{\text{diel}}$ ,  $\epsilon_i$  becomes unity. This appears at  $R_{\text{diel}} \approx 4 \text{ \AA}$  for  $\text{Ca}^{2+}$ , which coincides roughly with the upper radial limit of the empty space between the first and second coordination shells of water around the ion.<sup>33</sup> In other words, a smaller dielectric sphere cannot represent the dielectric depression of hydrated calcium ions experimentally determined. Finally, the estimation of  $\Delta\Delta F_c(E, R_{\text{diel}})$  trusts on the applicability of the continuum description of the excess ion hydration energy (given by eq 7) down to  $R_{\text{diel}}$ . Table 3 showed that this was the case down to  $6 \text{ \AA}$ , and hence we assume that this is reasonable even down to  $4\text{--}5 \text{ \AA}$ , although  $5 \text{ \AA}$  is a more natural limit for a divalent cation as polarization of its second coordination shell should still be treated as ion-specific.

An importance of the first peak of ion-oxygen distribution functions for properties of ions was demonstrated in ref 33, where it was stated that the effective Born radius of the energy of ion hydration could be identified as  $R_{\text{eff}} = (R_{\text{ion}} + R_{\text{gmax}})/2$ , where  $R_{\text{ion}}$  is the Goldschmidt ion radius and  $R_{\text{gmax}}$  is the radius of the first peak in ion-oxygen radial distribution function. This relation was verified for many anions and cations. It does not mean that any change of solvent permittivity caused by the electric field or by the increase of ion concentration should be substituted into the Born formula of the ion hydration energy taken with this effective radius  $R_{\text{eff}}$ . As follows from the present simulations, we can attribute an  $\epsilon(E)$  dependence starting from the second coordination shell, i.e., from about  $R_{\text{diel}} = 5 \text{ \AA}$ . Inside the ion hydration shell, the polarization should be an ion-specific function of  $E$ .

Beyond  $R_{\text{diel}}$ , the dependence of the local dielectric constant of water on the electric field and ion concentration is described

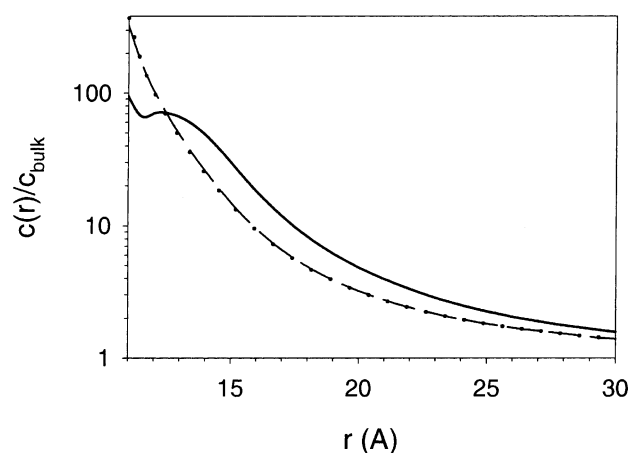


**Figure 5.** Radial concentration  $c(r)/c_{\text{bulk}}$  of calcium ion outside a charged cylinder representing DNA using the primitive polarization model (solid curve), the primitive polarization model but neglecting the excess ion hydration free energy (dotted curve), and the primitive model where the dielectric saturation of the solution is neglected (dashed curve); see text for further details.

by combining the Booth theory<sup>56</sup> and eq 9 according to

$$\epsilon(E, c) = \epsilon_w^{\text{Booth}}(E) - \sum_i \frac{\epsilon_w^{\text{Booth}}(E) - \epsilon_i}{\epsilon_w^{\text{Booth}}(0) - \epsilon_i} \delta_i(R_{\text{diel}}) c_i \quad (14)$$

where  $\delta_i(R_{\text{diel}})$  enters the equation. In other words, eq 14 constitutes a simple extension of eq 9 for dielectric saturation of water in the field  $E$  around the low dielectric cavity of the hydrated ion.

**Application to Ion Distributions Near DNA.** The significance of how the ion hydration free energy depends on the electrostatic field will be illustrated by examination of the distribution of calcium ions near DNA dissolved in an aqueous solution of  $0.0167 \text{ M CaCl}_2$  using the primitive polarization model.

A single DNA molecule is represented by an infinitely long and uniformly charged rod with radius  $7 \text{ \AA}$ , carrying one negative elementary charge per  $1.7 \text{ \AA}$  and possessing an interior relative permittivity of 2. The ions are described as charged hard spheres with radius  $2 \text{ \AA}$ , and the distance of the ion exclusion zone near DNA is  $4 \text{ \AA}$  (see below). Three cases of treating the dielectric polarization will be considered: (i) using the PPM with  $\delta_{\text{Ca}^{2+}} = 23 \text{ M}^{-1}$  and  $\delta_{\text{Cl}^-} = 3.5 \text{ M}^{-1}$ , which with  $R_{\text{diel}} = 4 \text{ \AA}$  gives  $\delta_{\text{Ca}^{2+}}(R_{\text{diel}}) = 15 \text{ M}^{-1}$  ( $\epsilon_{\text{Ca}^{2+}} = 2$ ) and  $\delta_{\text{Cl}^-}(R_{\text{diel}}) = 1.5 \text{ M}^{-1}$  ( $\epsilon_{\text{Cl}^-} = 2$ ), respectively; (ii) using the PPM but neglecting the excess free energy of polarization by assigning  $\Delta\Delta F_i(E) = 0$  (implying  $\delta_i = \delta_i(R_{\text{diel}}) = 0$ ) but retaining  $\epsilon(E, c) = \epsilon_w^{\text{Booth}}(E)$ ; and (iii) completely neglecting the dielectric saturation by assigning  $\Delta\Delta F_i(E) = 0$  and a uniform solution permittivity  $\epsilon(E, c) = \epsilon_w$ . Throughout, the low dielectric permittivity of DNA is retained.

The three cases were solved using the modified Poisson–Boltzmann (MPB) equations, and the mean electrostatic potential and ion distribution around DNA were determined. All the details of the MPB calculations were described in ref 47. Here we only notice that first case corresponds to eq 9 replaced by eq 14.

Figure 5 shows the relative calcium concentration near the DNA surface. In all cases, a strong accumulation of calcium ions near the DNA surface appears. By comparing cases (i) and (ii) (solid and dotted curves, respectively), we notify that the counterion distribution functions are notably affected by the



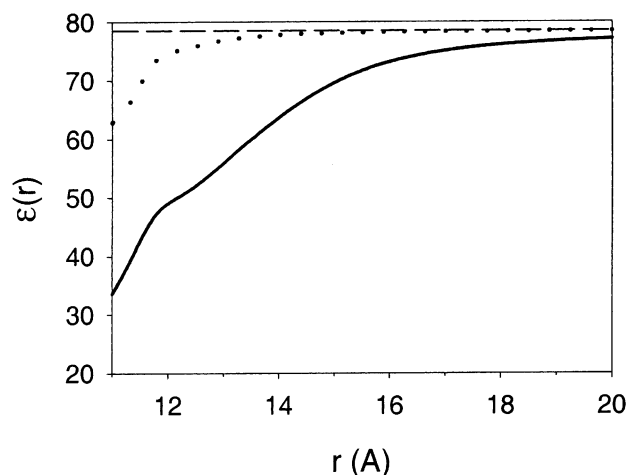


**Figure 6.** Relative water permittivity  $\epsilon(r)$  outside a charged cylinder representing DNA using the primitive polarization model (solid curve), the primitive polarization model but neglecting the excess ion hydration free energy (dotted curve), and the primitive model where the dielectric saturation of the solution is neglected (dashed curve); see text for further details.

polarization of ion hydration shells, but by comparison of cases (ii) and (iii) (dotted and dashed curves, respectively), the effect by the dielectric saturation of the solvent in the vicinity of the DNA by the electric field from the DNA is negligible. Hence, the PPM enables an additional repulsive force originating from the orientation polarization of the solvent to appear, which in the case investigated here reduces the  $\text{Ca}^{2+}$  concentration near the DNA surface.

The resulting relative solvent permittivity near the DNA is presented in Figure 6. Obviously a strong decrease of the relative permittivity near the DNA surface is predicted by the PPM, and the main effect arises from the dielectric saturation of the ion hydration shells.

Similar modeling, but with NaCl instead  $\text{CaCl}_2$ , have been performed. A much smaller difference of the counterion distribution near the DNA surface between the PPM (case i) and the PM (case iii) was obtained (data not shown). Hence, ion polarization and water dielectric saturation effects are concluded to be of less importance for monovalent counterions.

Thus, MPB results obtained with an improved model of the ion hydration cluster polarization confirm the conclusion stated in ref 47 that dielectric effects might play an important role in the electrostatics of DNA—a questionable subject since pioneering work by Skolnick and Fixman.<sup>66</sup> It is important to note that the applicability of our results relies on the rather arbitrary model of the ion exclusion zone around DNA and on the assumed 4 Å hard-sphere radius of the short-range interionic repulsion. The last value should be established more firmly by further explicit solvent simulations of effective interionic potentials. Usually the thickness of the ion exclusion zone is taken as 2–3 Å,<sup>47</sup> but here 4 Å was used to avoid significant overlap of the low-dielectric spheres of ions and low-dielectric interior of the rod. Such an overlap would be incompatible with the present formulation of the MPB equations. Nevertheless, our study illustrates the influence of the ion hydration shell polarization at longer distances where the PPM may be applied, and the obtained results suggest that the influence of the ion hydration shell polarization may not be neglected in this region.

## Conclusions

On the basis of Monte Carlo simulations, the polarization deficiency and the excess ion hydration free energy at an electric

field  $E$  (the ion hydration free energy at the field  $E$  subtracted by the ion hydration free energy at zero field) of hydrated calcium, sodium, and chloride ions have been determined. A spherical cell containing either one ion and molecular water or only molecular water subjected to different electric fields has been used. For pure water, the permittivity was found to decrease as  $E$  is increased in quantitative agreement with previous simulation studies and the Booth theory, verifying our approach. At fields up to ca. 0.025 V/Å, the excess hydration free energy depends quadratically on  $E$ , whereas it becomes linear in  $E$  at higher field due to dielectric saturation. The excess ion hydration free energies are in quantitative agreement with measured dependencies of the relative permittivity of electrolyte solution upon the ion concentration.

We also propose a primitive polarization model of electrolyte solution near charged interfaces, extending the primitive model of electrolyte solution by including the dielectric saturation of water by (i) the electric field from dissolved ions and (ii) an external electric field. The former effect is ion-specific and is described by representing the dielectric properties of an ion and approximately its first hydration shell by a dielectric sphere with a low permittivity deduced from experimental data or as here from simulations. The latter effect is accounted for by employing the Booth equation. We have shown that the radius of the dielectric sphere of a divalent cation such as  $\text{Ca}^{2+}$  cannot be less than 4 Å, and this model extension leads to an additional effective repulsion of hydrated ions near charged interfaces as compared to the primitive model. The distribution of calcium ions near a simple model of DNA is significantly affected, whereas the effect for monovalent counterions is small.

As well as introducing ion-specific long-range dispersion forces,<sup>25</sup> possible “classical” explanations of the ion-specific effects in highly charged systems should be investigated. There are at least three such effects that should be incorporated into a double layer theory describing such highly charged systems as bilayers and polyelectrolytes. The first is ion–water interactions close to the water-macromolecule interface. This highly ion-specific free energy contribution originates from molecular nature of solvent and might be significant, as it can be characterized in terms of work against the osmotic pressure of ionic gas in the area where local concentration of counterions reaches its maximum.<sup>67</sup> Only a few distribution functions of ions within this thin interfacial layer<sup>68,69</sup> have been studied in respect to various atomic groups,<sup>70</sup> and all these effective potentials can be revealed by further explicit solvent simulations. The second ion-specific effect can be roughly described by the radius of ion–ion hard-core interactions (or by a more detailed effective interionic potential taken from MD/MC simulations with explicit solvent molecules<sup>51,70</sup>). The hard-core radius of interionic interactions is treated as a hard-sphere diameter in the RPM and this parameter is sensitive for interionic correlation forces that cause such effects as overneutralization of multivalent RPM electrolyte at some distance from highly charged macromolecules.<sup>71</sup> The third ion-specific effect can be described as the size of the ion hydration shell and its polarization in an external electric field.

It should be noted that all three effects can be studied for different ions and specific ion-atomic group interactions by explicit solvent simulations for relatively small models.<sup>70</sup> Short-range ion-specific potentials of mean force together with spatially dependent dielectric properties of continuous solvent can be incorporated into an advanced statistical approach such

as the three-dimensional MPB equations to study large systems described on the level of all atom coordinates of a macromolecule.<sup>72</sup>

**Acknowledgment.** Financial support from the Swedish National Research Council (NFR) is gratefully acknowledged.

## References and Notes

- (1) Evans, D. F.; Wennerström, H. *The Colloidal Domain Where Physics, Chemistry and Technology Meet*; Wiley: New York, 1999.
- (2) Derjaguin, B. V.; Landau L. *Acta Physiochim. U.S.S.R.* **1941**, *14*, 633.
- (3) Verwey, E. J.; Overbeek, J. T. G. *Theory of the Stability of Lyophobic Colloids*; Elsevier: New York, 1948.
- (4) Khokhlov, A. R.; Zeldovich, K. B.; Kramarenko, E. Y. In *Counterions in Polyelectrolytes*; Holm, C., Kékicheff, P., Podgornik, R., Eds.; Kluwer Academic Press: London, 2001.
- (5) Bashford, D.; Karplus, M. *Biochemistry* **1990**, *29*, 10219.
- (6) Bashford, D.; Karplus, M. *J. Phys. Chem.* **1991**, *95*, 9556.
- (7) Takahashi, T.; Nakamura, H.; Wada, A. *Biopolymers* **1992**, *32*, 897.
- (8) Oberoi, H.; Allewell, N. M. *Biophys. J.* **1993**, *65*, 48.
- (9) Loewenthal, R.; Sancho, J.; Reinikainen, T.; Fersht, A. R. *J. Mol. Biol.* **1993**, *232*, 574.
- (10) Antosiewicz, J.; McCammon, J. A.; Gilson, M. K. *J. Mol. Biol.* **1994**, *238*, 415.
- (11) Kesvatera, T.; Jönsson, B.; Thulin, E.; Linse, S. *Biochemistry* **1994**, *33*, 14170.
- (12) Linse, S.; Jönsson, B.; Chaizin, W. J. *Proc. Natl. Acad. Sci. U.S.A.* **1995**, *92*, 4748.
- (13) Schaefer, M.; Sommer, M.; Karplus, M. *J. Phys. Chem. B* **1997**, *101*, 1663.
- (14) Grycuk, T. *J. Phys. Chem. B* **2002**, *106*, 1434.
- (15) Collins, K. D.; Washabaugh, M. W. *Quart. Rev. Biophys.* **1985**, *18*, 323.
- (16) Rau, D. C.; Parsegian, V. A. *Biophys. J.* **1992**, *61*, 246.
- (17) Sottas, P.-E.; Larquet, E.; Stasiak, A.; Dubochet, J. *Biophys. J.* **1999**, *77*, 1858.
- (18) Rau, D. C.; Lee, B.; Parsegian, V. A. *Proc. Natl. Acad. Sci. U.S.A.* **1984**, *81*, 2621.
- (19) Guldbrand, L.; Jönsson, B.; Wennerström, H.; Linse, P. *J. Chem. Phys.* **1984**, *80*, 2221.
- (20) Guldbrand, L.; Nilsson, L. G.; Nordenskiöld, L. *J. Chem. Phys.* **1986**, *85*, 6686.
- (21) Hribar, B.; Vlachy, V. *J. Phys. Chem. B* **1997**, *101*, 3457.
- (22) Lobaskin, V.; Linse, P. *Phys. Rev. Lett.* **1999**, *83*, 4208.
- (23) Allahyarov, E.; Löwen, H. *Phys. Rev. E* **2000**, *62*, 5542.
- (24) Gruen, D. W. R.; Marcelja, S. *J. Chem. Soc., Faraday Trans. 2* **1983**, *79*, 225.
- (25) Boström, M.; Williams, D. R. M.; Ninham, B. W. *J. Phys. Chem. B* **2002**, *106*, 7908.
- (26) Lamm, G.; Pack, G. R. *J. Phys. Chem. B* **1997**, *101*, 959.
- (27) Dang, L. X.; Rice, J. E.; Caldwell, J.; Kollman, P. A. *J. Am. Chem. Soc.* **1991**, *113*, 2481.
- (28) Dang, L. X.; Smith, D. E. *J. Chem. Phys.* **1993**, *99*, 6950.
- (29) Lee, S. H.; Rasaiah J. C. *J. Phys. Chem.* **1996**, *100*, 1420.
- (30) Raugei, S.; Klein, M. L. *J. Chem. Phys.* **2002**, *116*, 196.
- (31) Koneshan, S.; Rasaiah, J. C.; Lynden-Bell, R. M.; Lee, S. H. *J. Phys. Chem. B* **1998**, *102*, 4193.
- (32) Brodskaya, E.; Lyubartsev, A. P.; Laaksonen, A. *J. Chem. Phys.* **2002**, *116*, 7879.
- (33) Babu, C. S.; Lim, C. *J. Phys. Chem. B* **1999**, *103*, 7958.
- (34) Schwenk, C. F.; Loeffler, H. H.; Rode, B. M. *J. Chem. Phys.* **2001**, *115*, 10808.
- (35) Floris, F. M.; Tani, A. *J. Chem. Phys.* **2001**, *115*, 4750.
- (36) Zavitsas, A. A. *J. Phys. Chem. B* **2001**, *105*, 7805.
- (37) Kiselev, M.; Heinzinger, K. *J. Chem. Phys.* **1996**, *105*, 650.
- (38) Sandberg, L.; Edholm, O. *J. Chem. Phys.* **2002**, *116*, 2936.
- (39) Zaslavsky, A. Yu.; Svishchev, I. M. *J. Chem. Phys.* **2001**, *115*, 1448.
- (40) Hasted, J. B.; Ritson, D. M.; Collie, C. H. *J. Chem. Phys.* **1948**, *16*, 1.
- (41) Harris, F. E.; O'Konski, C. T. *J. Phys. Chem.* **1957**, *61*, 310.
- (42) Asaki, M. L. T.; Redondo, A.; Zawodzinski, T. A.; Taylor, A. J. *J. Chem. Phys.* **2002**, *116*, 8469.
- (43) Buchner, R.; Heftner, G. T.; May, P. M. *J. Phys. Chem. A* **1999**, *103*, 1.
- (44) Hubbard, J. B.; Onsager, L.; van Beek, W. M.; Mandel, M. *Proc. Natl. Acad. Sci. U.S.A.* **1977**, *74*, 401.
- (45) Bockris, J. O'M.; Reddy, A. K. N. In *Modern Electrochemistry*. V1, 2nd ed.; Plenum Press: New York, 1998.
- (46) Karlström, G. *J. Phys. Chem. B* **2002**, *106*, 5302.
- (47) Gavryushov, S.; Zielenkiewicz, P. *J. Phys. Chem. B* **1999**, *103*, 5860.
- (48) Böttcher, C. J. F. In *Theory of Electric Polarization*; Elsevier Scientific Publishing Company: Amsterdam, 1973.
- (49) Berendsen, H. J. C.; Grigera, J. R.; Straatsma, T. P. *J. Phys. Chem.* **1987**, *91*, 6269.
- (50) Åqvist, J. *J. Phys. Chem.* **1990**, *94*, 8021.
- (51) Smith, D. E.; Dang, L. X. *J. Chem. Phys.* **1994**, *100*, 3757.
- (52) Dang, L. X. *J. Am. Chem. Soc.* **1995**, *117*, 6954.
- (53) Linse, P. *MOLSIM, Ver. 3.0*; Lund University: Lund, Sweden, 2000.
- (54) Svishchev, I. M.; Kusalik P. G. *J. Phys. Chem.* **1994**, *98*, 728.
- (55) Yeh, I.-C.; Berkowitz, M. L. *J. Chem. Phys.* **1999**, *110*, 7935.
- (56) Booth, F. *J. Chem. Phys.* **1951**, *19*, 391/1327/1615.
- (57) Coker, H. *J. Phys. Chem.* **1976**, *80*, 2078.
- (58) Coker, H. *J. Phys. Chem.* **1976**, *80*, 2084.
- (59) Pyper, N. C.; Pike, C. G.; Edwards, P. P. *Mol. Phys.* **1992**, *76*, 353.
- (60) Chandra, A. *J. Chem. Phys.* **2000**, *113*, 903.
- (61) In the context of comparing experimental and simulated  $\delta_i$ , the difference between the relative permittivity at  $T = 298$  K of real water (78.5) and of the SPC/E water ( $\approx 70$ ) is of less importance as compared to the statistical uncertainties.
- (62) Prigogine, I.; Mazur, P.; Defay, R. *J. Chim. Phys.* **1953**, *50*, 146.
- (63) Bolt, G. H. *J. Colloid Sci.* **1955**, *10*, 206.
- (64) Sparnaay, M. J. *Rec. Trav. Chim. Pays-Bas* **1958**, *77*, 872.
- (65) Levine, S.; Bell, G. *Discuss. Faraday Soc.* **1966**, *42*, 69.
- (66) Skolnick, J.; Fixman, M. *Macromolecules* **1978**, *11*, 867.
- (67) Burak, Y.; Andelman, D. *J. Chem. Phys.* **2001**, *114*, 3271.
- (68) Rose, D. A.; Benjamin, I. *J. Chem. Phys.* **1993**, *98*, 2283.
- (69) Glosli, J. N.; Philpott, M. R. *J. Chem. Phys.* **1993**, *98*, 9995.
- (70) Lyubartsev, A. P.; Laaksonen, A. *J. Chem. Phys.* **1999**, *111*, 11207.
- (71) Abascal, J. L. F.; Montoro, J. C. G. *J. Chem. Phys.* **2001**, *114*, 4277.
- (72) Gavryushov, S.; Zielenkiewicz, P. *Biophys. J.* **1998**, *75*, 2732.